Journal of Inflammation Research

Dovepress
Taylor & Francis Group

Open Access Full Text Article

ORIGINAL RESEARCH

# Celastrol Mitigates Acute Pancreatitis Associated Inflammation by Modulating the IL-34/CSF-1R Axis and Suppressing NF-κB/ERK Signaling

Yang Yang[1], Xiangli Ma[1], Yujie Lin[1], Yue Mo[1], Yaoqi Xu[1], Bei Zhang[2], Xu Fu[3], Yingzhen Wang[1]

[1]Emergency Center, The Second Hospital & Clinical Medical School, Lanzhou University, Lanzhou City, Gansu, 730030, People's Republic of China; [2]Department of Critical Care Medicine, The Second Hospital & Clinical Medical School, Lanzhou University, Lanzhou City, Gansu, People's Republic of China; [3]Key Laboratory of Emergency Medicine, Second Hospital & Clinical Medical School, Lanzhou University, Lanzhou, People's Republic of China

Correspondence: Xu Fu, Key Laboratory of Emergency Medicine, The Second Hospital & Clinical Medical School, Lanzhou University, No. 82 Cuiyingmen, Chengguan District, Lanzhou City, Gansu, 730030, People's Republic of China, Email fuxu0910@163.com; Yingzhen Wang, Emergency Center, The Second Hospital & Clinical Medical School, Lanzhou University, No. 82 Cuiyingmen, Chengguan District, Lanzhou City, Gansu, 730030, People's Republic of China, Email ery_wangyzh@lzu.edu.cn



**Background:** Acute pancreatitis (AP) is characterized by early acinar injury followed by rapid inflammatory amplification, yet the upstream molecular triggers linking tissue stress to cytokine escalation remain incompletely defined. Interleukin-34 (IL-34), a ligand of colony-stimulating factor-1 receptor (CSF-1R), regulates inflammatory signaling, but its role in AP has not been elucidated. Celastrol is a bioactive triterpenoid with established anti-inflammatory properties; however, whether it modulates IL-34-associated signaling in AP remains unclear.

**Methods:** Experimental AP was induced in rats by retrograde sodium taurocholate infusion. Celastrol (6 mg/kg, i.p.) was administered 1 h prior to AP induction. In vitro, caerulein-stimulated AR42J acinar cells and IL-34 overexpressing cells were employed to evaluate functional relevance. ERK/NF-κB activation and inflammatory mediator production were assessed by Western blotting, ELISA, and immunofluorescence. Molecular docking was performed as an exploratory structural analysis of celastrol and the IL-34/CSF-1R complex.

**Results:** Celastrol significantly attenuated pancreatic injury in vivo, reducing serum amylase activity by approximately 34% and improving histological scores (both $P < 0.01$). IL-34 protein expression was markedly increased in experimental AP ($P < 0.001$), accompanied by activation of CSF-1R-dependent ERK and NF-κB signaling. IL-34 overexpression enhanced inflammatory outputs, whereas celastrol suppressed IL-34 expression and downstream signaling activation ($P < 0.05$). Docking analysis suggested structural compatibility between celastrol and IL-34/CSF-1R. Targeting IL-34 signaling may represent a potential therapeutic approach for acute pancreatitis.

**Conclusion:** These findings identify IL-34 as a previously unrecognized contributor to inflammatory amplification in experimental AP. Celastrol treatment was accompanied by reduced IL-34 expression and attenuation of ERK/NF-κB activation. Although further loss of function studies are required to establish direct causality, modulation of IL-34-related signaling may represent a potential therapeutic direction for AP.

**Keywords:** celastrol, NF-κB, ERK, IL-34, acute pancreatitis

## Introduction

Acute pancreatitis (AP) is a sterile inflammatory disorder initiated by premature intrapancreatic activation of digestive enzymes, leading to acinar injury and, in severe cases, systemic inflammatory response syndrome (SIRS) and multiple organ dysfunction syndrome (MODS).[1–3] Approximately 80% of patients experience a mild and self-limiting course, whereas nearly 20% progress to severe acute pancreatitis (SAP) with life-threatening complications.[4,5] Although advances in intensive care have reduced mortality, the global incidence of AP continues to rise.[4,5] Beyond the acute episode, AP confers substantial long-term morbidity, including recurrent hospitalizations, impaired quality of life, new-

https://doi.org/10.2147/JIR.S572609
Received: 23 October 2025
Accepted: 6 March 2026
Published: 12 March 2026

## Graphical Abstract

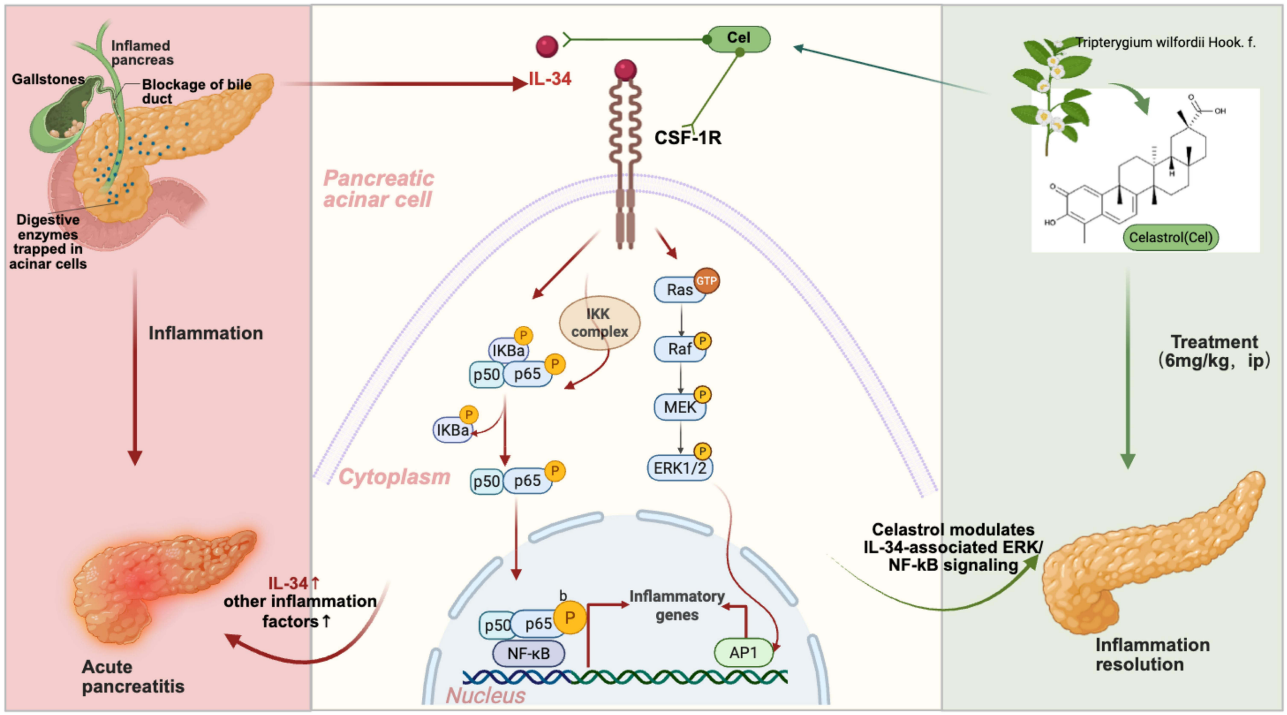


onset diabetes, and exocrine insufficiency.[4–6] Pancreatic inflammatory microenvironments are increasingly recognized as complex immunometabolic niches influencing disease progression.[7–10] Despite increasing mechanistic insight into inflammatory signaling pathways, clinical management remains largely supportive, and no targeted pharmacological therapy capable of interrupting early inflammatory amplification has been approved.[5,11–14]

The early phase of AP is characterized not only by acinar cell stress but also by rapid sterile immune activation. Damage-associated molecular patterns (DAMPs) released from injured acinar cells activate resident macrophages and recruit circulating leukocytes, initiating a cytokine amplification loop dominated by TNF-α, IL-6, and NF-κB-dependent transcriptional programs.[12–14] This feedforward inflammatory circuitry, rather than proteolytic injury alone, is increasingly recognized as a major determinant of disease severity and systemic complications.[13,14] Despite advances in supportive care, no targeted pharmacological intervention is currently available to interrupt this early inflammatory escalation. Consequently, identifying upstream cytokine receptor axes that bridge early acinar stress to sustained ERK/NF-κB activation is essential for the development of rational targeted therapies.

Interleukin-34 (IL-34) is a multifunctional cytokine that signals through the colony-stimulating factor-1 receptor (CSF-1R). Traditionally recognized for its role in macrophage survival and differentiation,[15–19] IL-34 has recently been implicated in several sterile inflammatory disorders.[20] Activation of CSF-1R triggers downstream MEK–ERK and NF-κB signaling cascades, promoting transcription of pro-inflammatory mediators.[19,21] Given that monocytes and macrophages are central mediators of early systemic inflammation in AP,[1,14] IL-34 may represent a potential upstream regulator of CSF-1R/ERK–dependent inflammatory signaling. To date, however, IL-34 expression and signaling dynamics have not been systematically examined in experimental models of AP. Notably, although CSF-1R is predominantly expressed in myeloid cells, emerging evidence suggests inducible expression in certain epithelial and non-hematopoietic cells under inflammatory stress,[21–23] raising the possibility that IL-34 may directly influence pancreatic acinar cells during AP.

Celastrol, a bioactive triterpenoid extracted from Tripterygium wilfordii Hook. F., has demonstrated protective effects across multiple sterile inflammatory conditions, including autoimmune hepatitis and rheumatoid arthritis.[24–26]

Mechanistically, celastrol suppresses convergent inflammatory nodes, including ERK and NF-κB signaling pathways.[27] Because these pathways are critically engaged during early inflammatory amplification in AP, celastrol represents a biologically plausible candidate for modulating pancreatic inflammation. However, whether its protective effects in AP involve regulation of the IL-34/CSF-1R axis remains unknown.

Based on these considerations, we hypothesized that IL-34 contributes to inflammatory amplification in AP through activation of the CSF-1R/ERK/NF-κB pathway and that celastrol mitigates pancreatic injury, at least in part, by modulating IL-34-associated signaling.

## Aim of the Study

The present study aimed to determine whether celastrol alleviates pancreatic injury and inflammatory responses in experimental AP. We further sought to characterize IL-34 expression dynamics during AP and to investigate whether IL-34 is associated with activation of the CSF-1R/ERK/NF-κB signaling pathway. By establishing an IL-34 overexpressing AR42J cell model, we aimed to provide gain of function evidence supporting the functional contribution of IL-34 to acinar inflammatory activation. Finally, we evaluated whether the protective effects of celastrol are mediated, at least in part, through modulation of IL-34-associated signaling.

# Materials and Methods

## Animals and Experimental AP Model

Male specific pathogen-free Sprague–Dawley rats (8 weeks old, ~260 g) were obtained from the Lanzhou Institute of Veterinary Research [license No. SCXK (Gan) 2020–0002]. Animals were housed under standard laboratory conditions (23 ± 2 °C; 50–60% humidity; 12 h light/dark cycle) with free access to food and water. All procedures were approved by the Animal Care and Use Committee of the Second Hospital of Lanzhou University (approval No. D2024-227) and conducted in accordance with ARRIVE guidelines.

Celastrol (purity ≥98%) was obtained from MedChemExpress (Cat. No. HY-13067). Celastrol is a quinone methide triterpenoid derived from Tripterygium wilfordii Hook. F. Stock solutions were prepared in DMSO and diluted to working concentrations in culture medium or saline immediately prior to use.

AP was induced by retrograde infusion of 3.5% sodium taurocholate (Sigma, T4009) into the pancreatic duct (1 mL/kg over 4 min). Rats received celastrol (6 mg/kg, i.p.) 1 h prior to AP induction to model preventive modulation of early inflammatory signaling, as cytokine amplification occurs within hours after induction. This dosing regimen was selected based on previous experimental studies.[28,29] Animals were randomly assigned to groups. Postoperative analgesia was provided using buprenorphine (0.05 mg/kg, s.c.). Prespecified exclusion criteria were established prior to the experiment to ensure data integrity. Animals were excluded from analysis if any of the following occurred: (1) unsuccessful ductal cannulation or evident leakage of sodium taurocholate into the peritoneal cavity during infusion; (2) death within 24 h post-surgery prior to the scheduled euthanasia; (3) signs of severe postoperative distress or infection not alleviated by analgesia, as determined by the institutional veterinary staff. Twenty-four hours after AP induction, rats were euthanized with pentobarbital sodium (40 mg/kg, i.p.), and serum and pancreatic tissues were collected.

## Cell Lines

AR42J rat pancreatic acinar cells were cultured in F12K medium (Procell, CM-0025) supplemented with 20% fetal bovine serum at 37 °C in 5% $CO_2$. To induce acinar-like differentiation, cells were treated with dexamethasone (Solarbio, D8040) for 48 h. After differentiation, cells were stimulated with caerulein (100 nM; MCE, HY-A0190) for 24 h to establish an in vitro AP model.

For pharmacological intervention studies, cells were pretreated with celastrol (2.0 μM), PD98059 (10 μM; MCE, HY-12028), or PDTC (60 μM; MCE, HY-18738) for 1 h prior to caerulein stimulation, without removing the inhibitors. This pretreatment-only design was selected to model preventive inhibition of early signaling activation, as ERK/NF-κB phosphorylation occurs rapidly after caerulein exposure. Celastrol was dissolved in DMSO, and the final DMSO

concentration did not exceed 0.1% (v/v). AR42J cells between passages 5–15 were used. Cells were seeded at $4 \times 10^5$ cells per well in 6-well plates.

## Real-Time Quantitative PCR (RT-qPCR)

Total RNA was isolated from cells with a kit following the manufacturer's protocol, and 1 μg of RNA was reverse transcribed to generate cDNA. Real-time PCR was conducted on a LightCycler® instrument using AceQ qPCR SYBR Green Master Mix. The reaction conditions were as follows: initial predenaturation at 95°C for 5 min, followed by 40 cycles of denaturation at 95°C for 10s and annealing and extension at 60°C for 30s. GAPDH, which is stably expressed in AR42J cells and pancreatic tissue, was used as an internal control gene for RT–qPCR analysis of target genes in the samples. In this study, GAPDH was selected as the reference gene, and the expression of the target genes was normalized to that of GAPDH. Relative expression levels were calculated using the 2−ΔΔCt method. The sequences of the primer pairs were as follows: IL-34 forward: 5′-TGCTGCAAACAAAGTCCCATC-3′ and reverse: 5′: GTACACGTTGGTAGCTGCACATT-3′; and GAPDH forward: 5′- CTGGAGAAACCTGCCAAGTATG-3′ and reverse: 5′-GGTGGAAGAATGGGAGTTGCT-3′.

## Western Blot Analysis

Pancreatic tissue and AR42J cells were lysed in RIPA lysis buffer. Proteins were extracted from the pancreatic tissues of 6 rats per group, or lysates were prepared for three independent cell culture experiments. The proteins were then separated by SDS-PAGE and transferred to a PVDF membrane (Millipore, IPVH00010). After blocking, the membranes were incubated overnight at 4 °C with the following primary antibodies: anti–IL-34 (Boster, A06903-3, 1:1000), anti–CSF-1R (Huaan Biotechnology, HA723142, 1:2000), anti–phospho-p65 (Huaan Biotechnology, HA723223, 1:5000), anti–phospho-ERK1/2 (Huaan Biotechnology, ET1610-13, 1:5000), and anti-GAPDH (Bioss, bs-10900R, 1:10,000). Subsequently, specific binding was detected using corresponding secondary antibodies. Immunoreactive bands were detected using an ECL Advanced Western Blotting Detection Kit and visualized with the Tanon Imaging System. The apparent molecular weight of IL-34 (~45 kDa) corresponds to the mature glycosylated form, consistent with previous reports.[30,31] Band intensities were quantified using ImageJ software (NIH, USA). Target protein expression was normalized to GAPDH and expressed as fold change relative to the control group. Quantification was performed on at least three independent experiments.

## Enzyme-Linked Immunosorbent Assay (ELISA)

The concentrations of TNF-α, IL-6, and IL-34 in serum and cell supernatants were determined using commercially available ELISA kits (Ruixinbio, China, Catalog: IL-34: RX2D374986, IL-6: RX2D302196, TNF-α: RX2D310636), following the manufacturer's instructions. Each sample was tested in triplicate, and absorbance was measured at 450 nm. Experiments were independently repeated three times. This protocol was adapted from previously published methods.[32] The detection ranges of ELISA kits were as follows: TNF-α (10–320 pg/mL, sensitivity<1.0 pg/mL), IL-6 (5–160 pg/mL, sensitivity<1.0 pg/mL), and IL-34 (50–1600 pg/mL, sensitivity<10.0 pg/mL). All samples were measured within the linear range of the standard curve.

## Histopathology and Statistical Analysis

The pancreas was dissected and washed with PBS. The specimens were fixed in formalin, embedded in paraffin, sectioned into 3 μm slices, and stained with H&E. The severity of pancreatic inflammation was graded through histological evaluation using a previously described scoring system[33] in a blinded manner. The severity of pancreatic injury was evaluated in a blinded manner using a standardized histological scoring system. The scoring parameters included interstitial edema, inflammatory cell infiltration, acinar necrosis, and hemorrhage. Each parameter was graded on a scale of 0–4 based on the extent of tissue involvement (0 = absent; 1 = minimal; 2 = mild; 3 = moderate; 4 = severe). For each animal, three non-overlapping high-power fields were randomly selected, and the average score was used for statistical analysis. A higher cumulative score indicated more severe pancreatic injury.

## Construction of a Stable IL-34 Overexpressing AR42J Cell Line

Rat pancreatic acinar AR42J cells were transduced with a lentiviral vector encoding full-length rat IL-34 (NM_001025766.1) fused to a C-terminal 3×Flag tag and a puromycin resistance cassette (pLenti-SFFV-IL-34-3Flag-P2A-Puro; GeneCarer, China). Recombinant lentivirus was packaged in HEK293T cells using a second-generation packaging system (psPAX2 and pMD2. G plasmids) according to the manufacturer's instructions.

AR42J cells were infected at a multiplicity of infection (MOI) of 10 in the presence of 5 μg/mL polybrene to enhance transduction efficiency. After 48 h, cells were selected with 2 μg/mL puromycin for 7 days to establish a stable IL-34 overexpressing (OE) cell line. Transduction efficiency was initially monitored by fluorescence microscopy based on the co-expressed EGFP reporter. Overexpression of IL-34 was further confirmed by quantitative real-time PCR and IF staining. Cells transduced with empty vector lentivirus served as vector controls, and non-transduced AR42J cells were used as additional baseline controls where indicated.

## Immunofluorescence (IF)

Cells or paraffin sections were incubated with primary antibodies against IL-34 (Thermo Fisher Scientific, PA5-95624, 1:200), p-ERK1/2 (1:200), or pp65 (1:200) overnight at 4 °C. Alexa Fluor 488- or 594-conjugated secondary antibodies (Abcam, ab150077 and ab150080, 1:500) were applied for 1 h at room temperature. Nuclei were counterstained with DAPI (Beyotime, China). Images were captured using a Zeiss LSM 880 confocal microscope. This protocol was adapted from established procedures with minor modifications.[34]

For double immunofluorescence staining of pancreatic tissue, paraffin-embedded sections were deparaffinized, rehydrated, and subjected to antigen retrieval in citrate buffer (pH 6.0). After blocking with 5% bovine serum albumin for 1 h at room temperature, sections were incubated overnight at 4 °C with primary antibodies against CSF-1R (1:200) and amylase (Proteintech, 12540-1-AP, 1:200) raised in different host species. After washing with PBS, sections were incubated with species-specific Alexa Fluor 488- and Alexa Fluor 594-conjugated secondary antibodies for 1 h at room temperature in the dark. Nuclei were counterstained with DAPI. Negative controls were processed in parallel by omitting primary antibodies to exclude non-specific secondary antibody binding. Representative merged images were generated to assess spatial co-localization.

## Immunohistochemistry (IHC)

Immunohistochemistry was conducted on 3-μm paraffin sections of pancreatic tissue using primary antibodies against IL-34 (1:200), p-ERK1/2 (1:200), and pp65 (1:200). DAB substrate was used for color development, and nuclei were counterstained with hematoxylin. Staining intensity was quantified using ImageJ. The protocol was modified from previous studies.[34]

## Instrumentation and Equipment

The following analytical instruments were employed for data acquisition and analysis: LightCycler® 480 Real-Time PCR System (Roche, Switzerland); Zeiss LSM 880 Confocal Microscope (Carl Zeiss, Germany); Leica DM2500 Light Microscope (Leica Microsystems, Germany); BioTek Synergy H1 Microplate Reader (BioTek Instruments, USA); Tanon 5200 Chemiluminescence Imaging System (Tanon, China).

## Statistical Analysis

Statistical analyses were performed using GraphPad Prism version 9.0 (GraphPad Software, San Diego, CA, USA). Normality of data distribution was assessed using the Shapiro–Wilk test, and homogeneity of variances was evaluated using Levene's test. For data meeting parametric assumptions, comparisons between two groups were performed using an unpaired Student's *t*-test, and comparisons among multiple groups were conducted using one-way analysis of variance (ANOVA) followed by Tukey's multiple comparisons test. For experiments involving two independent variables, two-way ANOVA was used to evaluate main effects and interaction effects, followed by Tukey's multiple comparisons test where appropriate. When data did not meet the assumptions of normality or homogeneity of variance, non-parametric

tests were applied (Mann–Whitney *U*-test for two-group comparisons or Kruskal–Wallis test followed by Dunn's multiple comparisons test for multiple groups). ANOVA results are reported as F values with corresponding P values. Data are presented as mean ± standard deviation (SD). For in vivo experiments, n represents the number of animals per group; for in vitro experiments, n represents independent biological replicates. All tests were two-tailed, and a P value < 0.05 was considered statistically significant.

# Results

## Celastrol Attenuates Pancreatic Injury and Inflammatory Mediator Release in vivo and Reduces Acinar Inflammatory Outputs in vitro

Histopathological examination revealed extensive pancreatic edema, inflammatory cell infiltration, and acinar structural disruption in AP rats compared with sham controls (Figure 1A). Because histological scores failed the Shapiro–Wilk normality test, non-parametric analysis was applied. Kruskal–Wallis testing demonstrated significant differences among groups ($P < 0.001$), with the celastrol-treated group exhibiting a partial but significant reduction in injury severity compared with AP animals. Consistent with histological improvement, serum amylase activity was markedly elevated in AP rats and significantly decreased following celastrol pretreatment (Figure 1B; one-way ANOVA, $F(2,15) = 17.62$, $P < 0.001$). Systemic inflammatory activation was similarly observed. Serum TNF-α and IL-6 concentrations were significantly increased in AP animals and reduced after celastrol administration (Figure 1C; TNF-α: $F(2,15) = 22.66$, $P < 0.001$; IL-6: $F(2,15) = 23.56$, $P < 0.001$).

In vitro, caerulein-stimulated AR42J cells recapitulated acinar inflammatory activation. Pharmacological inhibition of ERK (PD98059), NF-κB (PDTC), or treatment with celastrol significantly reduced supernatant amylase activity (Figure 1D; one-way ANOVA, $F(4,10) = 20.39$, $P < 0.001$) and suppressed cytokine release (Figure 1E; IL-6: $F(4,10) = 25.15$, $P < 0.001$; TNF-α: $F(4,10) = 10.94$, $P = 0.001$). Together, these in vivo and in vitro findings indicate that celastrol blunts early AP-associated inflammatory amplification, as reflected by reduced acinar injury markers and systemic cytokine release.

## IL-34 Protein Expression is Elevated During AP and Reduced by Celastrol

Western blot analysis demonstrated significantly increased IL-34 protein expression in pancreatic tissue from AP rats compared with sham controls (Figure 2A; one-way ANOVA, $F(2,6) = 19.26$, $P = 0.002$), with a significant reduction following celastrol pretreatment (Tukey post-hoc $P < 0.01$ vs AP). Circulating IL-34 levels mirrored tissue protein changes. Serum IL-34 was markedly elevated in AP rats and decreased in celastrol-treated animals (Figure 2B; $F(2,15) = 32.69$, $P < 0.001$). Immunohistochemical analysis further confirmed enhanced IL-34 immunoreactivity within pancreatic parenchyma in AP animals, which was attenuated after celastrol administration (Figure 2C; $F(2,6) = 186.3$, $P < 0.001$).

In AR42J cells, caerulein stimulation significantly increased IL-34 protein abundance. One-way ANOVA demonstrated significant treatment effects (PD98059 set: $F(3,8) = 13.31$, $P = 0.002$; PDTC set: $F(3,8) = 11.32$, $P = 0.003$). ERK inhibition, NF-κB inhibition, and celastrol treatment each reduced IL-34 protein levels relative to AP conditions (Figure 2D). These data establish that IL-34 protein is induced during experimental AP and is modifiable by celastrol.

## CSF-1R Associated ERK/NF-κB Signaling is Activated During AP and Attenuated by Celastrol

Double immunofluorescence staining demonstrated spatial colocalization of CSF-1R immunoreactivity with amylase-positive acinar structures in pancreatic tissue (Figure 3A), indicating that CSF-1R expression may be detectable within or in close proximity to acinar cells under inflammatory conditions. However, contributions from infiltrating myeloid populations cannot be excluded based solely on colocalization analysis.

In vivo, Western blot analysis revealed significant upregulation of CSF-1R expression in AP tissue, accompanied by increased phosphorylation of p65 and ERK1/2 (Figure 3B; CSF-1R: $F(2,6) = 18.04$, $P = 0.003$; pp65: $F(2,6) = 73.04$, $P < 0.001$; p-ERK1/2: $F(2,6) = 11.49$, $P = 0.009$). Celastrol pretreatment significantly reduced these signaling markers.

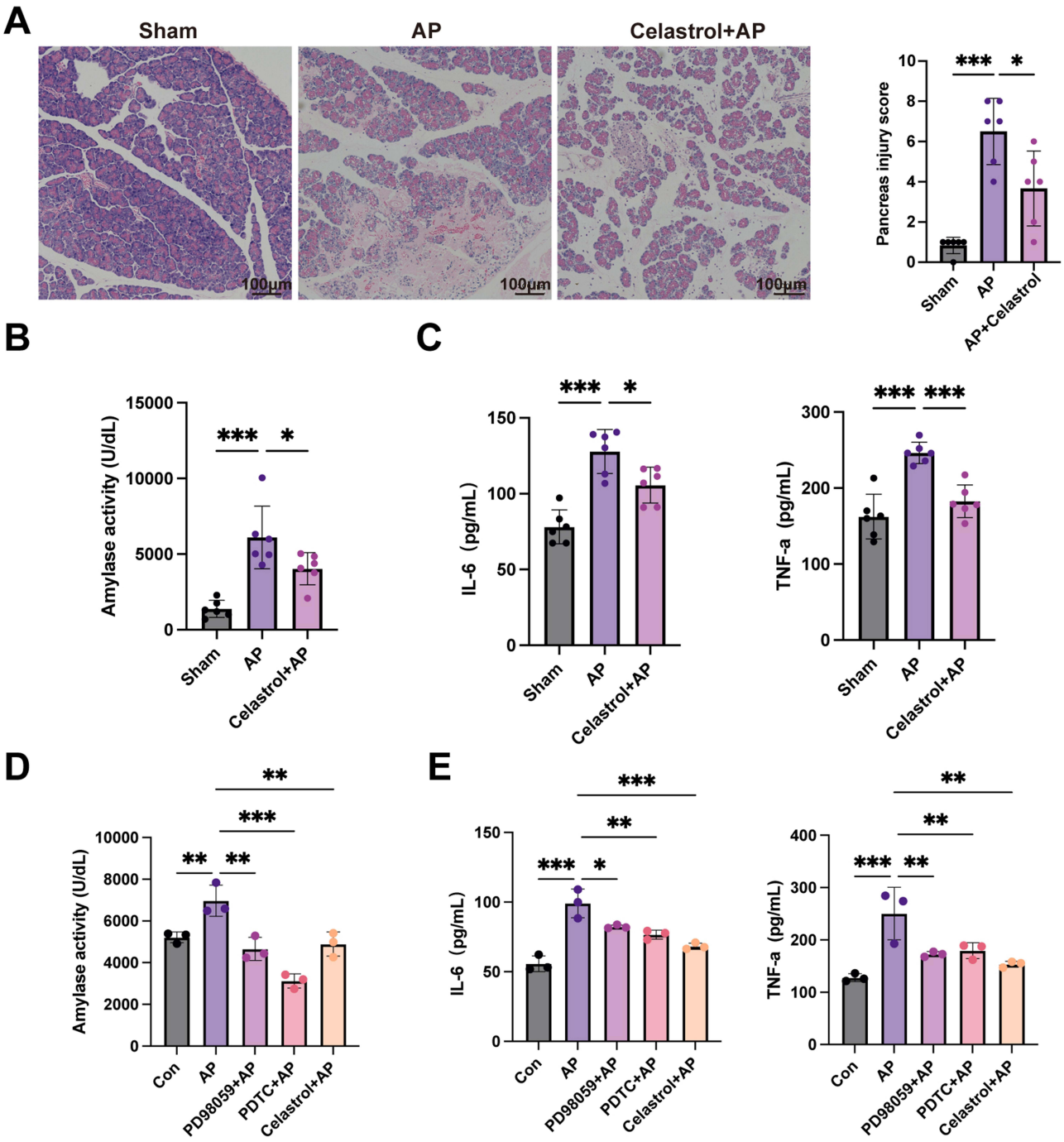


**Figure 1** Celastrol attenuates pancreatic injury and inflammatory mediator release in experimental AP. (**A**) Representative H&E staining of pancreatic tissue from Sham, AP, and Celastrol+AP rats with corresponding histological injury scores (scale bar: 100 μm). (**B**) Serum amylase levels (n = 6 rats per group). (**C**) Serum IL-6 and TNF-α levels measured by ELISA (n = 6 rats per group). (**D**) Amylase activity in AR42J cell supernatants under Con (Control), AP (caerulein), and AP plus PD98059, PDTC, or celastrol treatment (n=3 independent experiments). (**E**) IL-6 and TNF-α levels in AR42J cell supernatants (n = 3 independent experiments). Data are presented as mean ± SD. Each dot represents an individual animal or independent experiment. Statistical analysis was performed using one-way ANOVA for data in (**B–E**) with Tukey's post-hoc test, except for histological scores in (**A**), which were analyzed by Kruskal–Wallis test. *P < 0.05, **P < 0.01, ***P < 0.001 vs AP group.

In AR42J cells, caerulein stimulation increased CSF-1R expression and activated ERK/NF-κB signaling (Figure 3C and D). Significant group effects were observed (CSF-1R: PD98059 set $F(3,8) = 82.26$, $P < 0.001$; PDTC set $F(3,8) = 9.01$, $P = 0.006$). Downstream signaling activation was likewise significant (PD98059 set: pp65 $F(3,8) = 24.50$, $P < 0.001$; p-ERK1/2 $F(3,8) = 31.93$, $P < 0.001$; PDTC set: pp65 $F(3,8) = 34.84$, $P < 0.001$; p-ERK1/2 $F(3,8) = 27.69$, $P <$


https://doi.org/10.2147/JIR.S572609

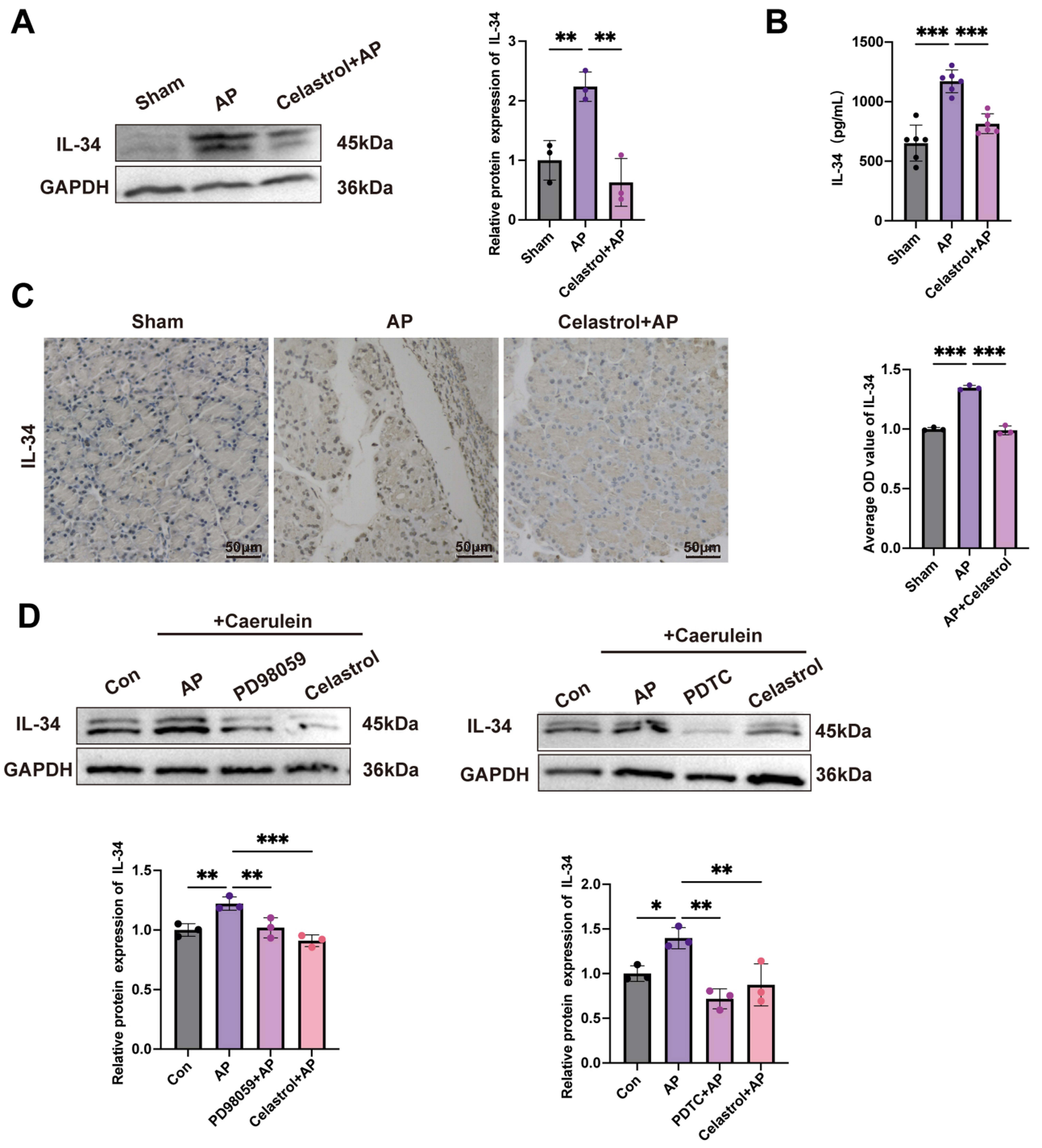


**Figure 2** IL-34 expression is increased in experimental AP and reduced by celastrol treatment. (**A**) Western blot analysis of IL-34 in pancreatic tissue with densitometric quantification normalized to GAPDH (n = 3 independent biological replicates). (**B**) Serum IL-34 levels measured by ELISA (n = 6 rats per group). (**C**) Representative immunohistochemical staining of IL-34 in pancreatic sections with quantitative analysis (scale bar: 50 μm; n = 6 rats per group). (**D**) Western blot analysis of IL-34 in AR42J cells under Con, AP, and AP plus PD98059, PDTC, or celastrol treatment (n = 3 independent biological replicates). Data are presented as mean ± SD. *P < 0.05, **P < 0.01, ***P < 0.001 vs AP group.

0.001). Across all conditions, celastrol attenuated CSF-1R expression and downstream pathway activation. Together, these findings indicate that CSF-1R-associated ERK/NF-κB signaling is induced during AP and is sensitive to celastrol intervention.

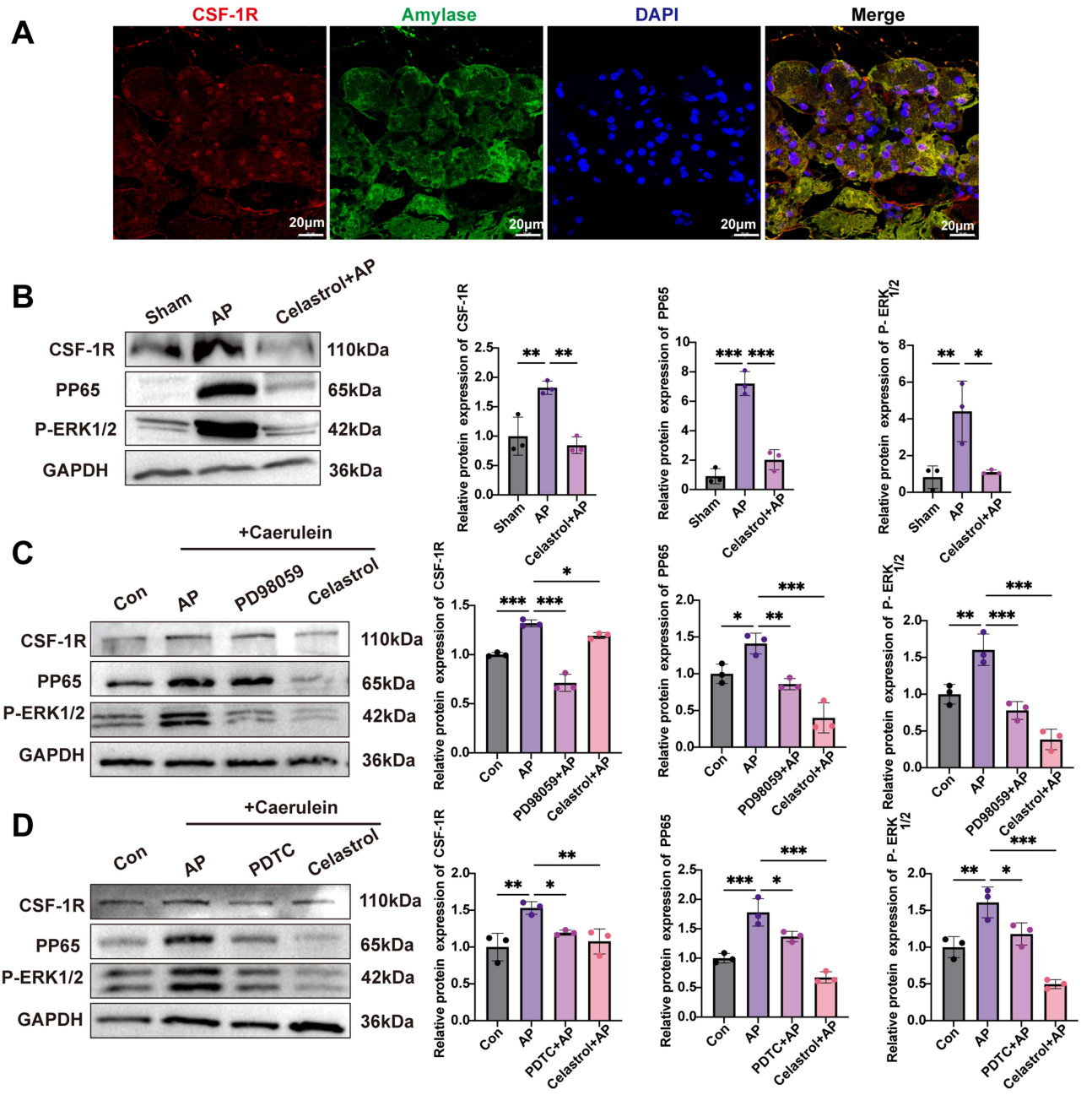


**Figure 3** CSF-1R–associated ERK/NF-κB signaling is activated during AP and modulated by celastrol. (**A**) Representative double immunofluorescence staining of CSF-1R (red) and amylase (green) in pancreatic tissue with DAPI nuclear counterstaining (blue). Colocalization indicates spatial association under inflammatory conditions (scale bar: 20 μm). (**B**) Western blot analysis of CSF-1R, p-ERK1/2, and p-p65 in pancreatic tissue (n = 3 independent biological replicates). (**C** and **D**) Western blot analysis of CSF-1R, p-ERK1/2, and p-p65 in AR42J cells under Con, AP, and AP plus PD98059, PDTC, or celastrol treatment (n = 3 independent biological replicates). The two closely migrating bands detected for p-ERK correspond to the phosphorylated forms of ERK1 (44 kDa) and ERK2 (42 kDa). Data are presented as mean ± SD. *P < 0.05, **P < 0.01, ***P < 0.001 vs AP group.

## IL-34 Overexpression Amplifies Inflammatory Activation in Acinar Cells and Remains Suppressible by Celastrol Under AP-Like Conditions

A stable IL-34 overexpressing (OE) AR42J cell line was successfully established and validated by qPCR (Figure 4A; unpaired *t*-test, P < 0.001) and immunofluorescence (Figure 4B), confirming robust elevation of IL-34 expression. Compared with WT cells, IL-34 OE significantly increased amylase release (Figure 4C; P < 0.05) and enhanced secretion of TNF-α and IL-6 (Figure 4D; both P < 0.01), indicating that elevated IL-34 is sufficient to augment inflammatory


https://doi.org/10.2147/JIR.S572609

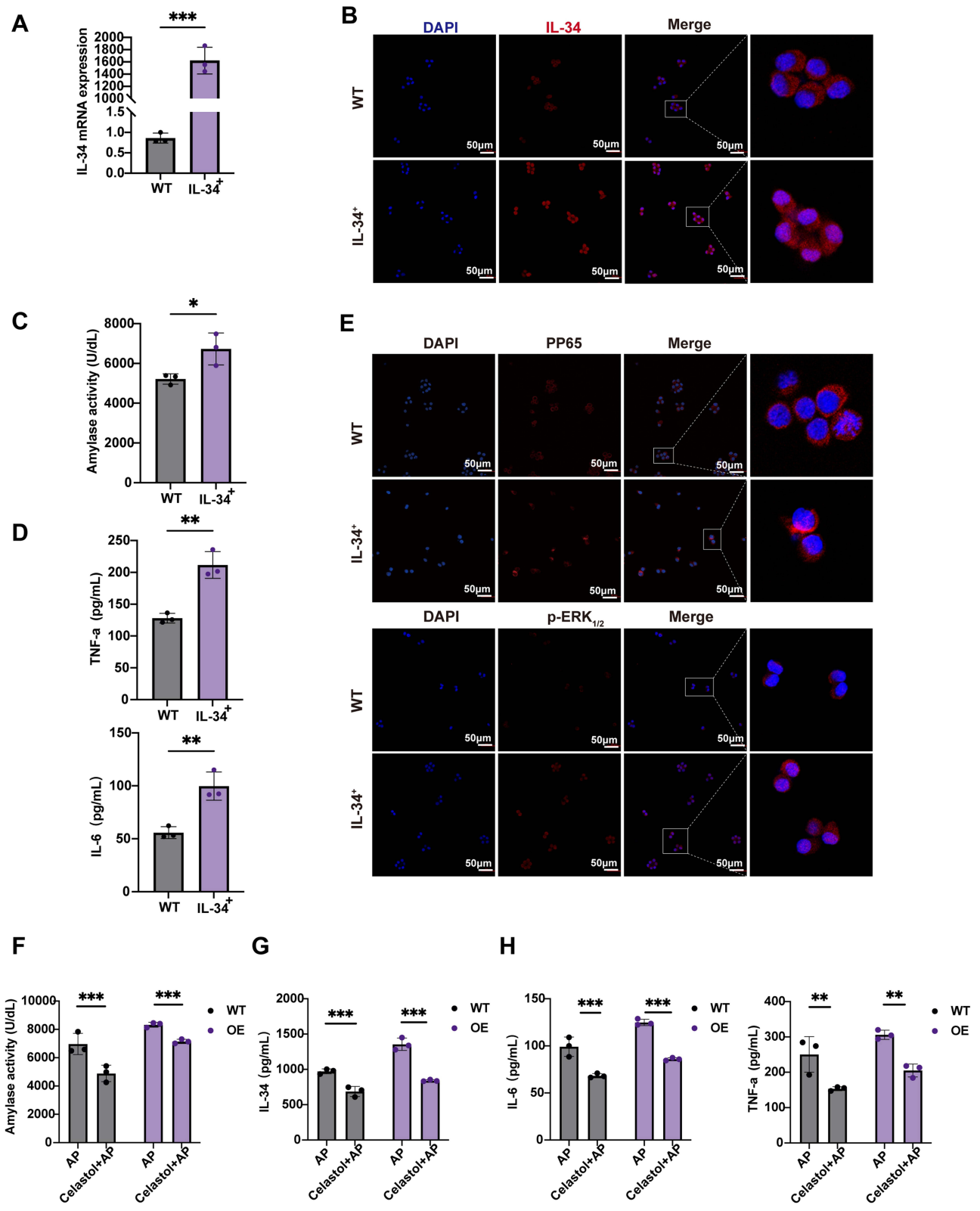


**Figure 4** IL-34 overexpression enhances inflammatory responses and modulates sensitivity to celastrol in AR42J cells. (**A**) Validation of IL-34 overexpression by qPCR. (**B**) Immunofluorescence confirmation of IL-34 overexpression (scale bar: 50 μm). (**C**) Amylase levels in Wild-type (WT) and IL-34-overexpressing (OE) cells (n = 3 independent experiments). (**D**) TNF-α and IL-6 levels in WT and OE cells (n = 3 independent experiments). (**E**) Immunofluorescence staining of pp65 and p-ERK in WT and OE cells (scale bar: 50 μm). (**F–H**) Two-way ANOVA analysis of amylase, IL-34, IL-6, and TNF-α levels. Data are presented as mean ± SD (n=3 independent experiments). (**F**) Amylase, (**G**) IL-34, and (**H**) TNF-α and IL-6 levels in WT and OE cells under indicated conditions. Data were analyzed by two-way ANOVA (genotype × treatment). Significant main effects of genotype and treatment were observed for all cytokines; a significant interaction term was found for IL-34 secretion (P = 0.01), indicating genotype-dependent modulation. Statistical significance is indicated as *P < 0.05, **P < 0.01, ***P < 0.001 compared to the respective AP control groups within each genotype.


https://doi.org/10.2147/JIR.S572609

output in acinar cells. Consistently, immunofluorescence analysis demonstrated enhanced nuclear localization of p65 and increased p-ERK fluorescence intensity in IL-34 OE cells relative to WT controls (Figure 4E), supporting activation of downstream ERK/NF-κB signaling in response to IL-34 overexpression.

To determine whether celastrol could suppress inflammatory responses under conditions of elevated IL-34, two-way ANOVA (genotype × treatment) was performed using WT and OE cells stimulated with AP ± celastrol. For amylase activity (Figure 4F), significant main effects were observed for genotype ($F(1,8) = 41.37$, $P = 0.0002$) and treatment ($F(1,8) = 33.44$, $P = 0.0004$), with no significant interaction effect ($F(1,8) = 2.54$, $P = 0.1498$). Post-hoc comparisons confirmed that celastrol significantly reduced amylase activity in both WT and OE cells under AP stimulation. For IL-34 secretion (Figure 4G), both genotype ($F(1,8) = 61.60$, $P < 0.0001$) and treatment ($F(1,8) = 136.40$, $P < 0.0001$) showed significant main effects, with a significant interaction term ($F(1,8) = 11.24$, $P = 0.0100$), indicating genotype-dependent modulation of celastrol responsiveness. Similarly, IL-6 secretion (Figure 4H) was significantly influenced by genotype ($F(1,8) = 44.99$, $P = 0.0002$) and treatment ($F(1,8) = 117.00$, $P < 0.0001$). TNF-α levels were also significantly affected by genotype ($F(1,8) = 11.29$, $P = 0.0099$) and treatment ($F(1,8) = 38.47$, $P = 0.0003$). In both cases, celastrol significantly reduced cytokine release under AP conditions regardless of genotype.

Collectively, these findings demonstrate that IL-34 overexpression enhances acinar inflammatory activation and downstream ERK/NF-κB signaling, while celastrol retains measurable anti-inflammatory efficacy even in the context of heightened IL-34 signaling.

## Discussion

The pathological progression of AP begins with premature intra-acinar activation of digestive enzymes, followed by rapid inflammatory amplification that largely determines systemic progression and clinical severity.[1,35] Despite improvements in supportive care, targeted pharmacological interventions capable of modulating early inflammatory signaling remain limited.[2] Identifying upstream cytokine networks that sustain acinar-associated inflammatory escalation therefore has important mechanistic and translational implications.[5,8] In this context, the present study implicates the IL-34/CSF-1R axis as a contributor to inflammatory amplification in experimental AP and demonstrates that celastrol attenuates pancreatic injury and inflammatory outputs in association with modulation of this signaling cascade.

In vivo, celastrol partially improved histopathological injury and reduced serum amylase, TNF-α, and IL-6 levels (Figure 1A–C), while in vitro it suppressed amylase release and cytokine production in caerulein-stimulated AR42J cells (Figure 1D and E). These findings are consistent with prior studies demonstrating the anti-inflammatory properties of celastrol in diverse inflammatory models.[25,36,37]

A central observation is the marked induction of IL-34 protein during experimental AP. IL-34, an alternative ligand for CSF-1R, has been primarily characterized in the regulation of myeloid lineage survival and differentiation.[15,18,19] Increasing evidence suggests that IL-34 participates in chronic inflammatory and autoimmune disorders,[20,38] and may exacerbate inflammatory tissue injury.[39] The present study extends these observations to sterile pancreatic inflammation, showing elevated IL-34 protein in pancreatic tissue and caerulein-stimulated acinar cells, with corresponding increases in circulating IL-34 (Figure 2A–2C). In AR42J cells, ERK inhibition (PD98059), NF-κB inhibition (PDTC), and celastrol each reduced IL-34 protein abundance (Figure 2D), suggesting that IL-34 induction is embedded within ERK/NF-κB responsive signaling networks, consistent with previous mechanistic studies.[19,32] These findings support the interpretation that IL-34 may function as an inducible inflammatory amplifier rather than a passive biomarker of tissue damage.[17]

CSF-1R associated signaling was likewise enhanced during AP. Increased CSF-1R expression and phosphorylation of ERK1/2 and p65 were detected in pancreatic tissue (Figure 3B), with similar activation observed in AR42J cells (Figure 3C and D). Although CSF-1R is classically associated with the mononuclear phagocyte system,[18] inducible expression in epithelial or tumor-derived cells has been reported under pathological conditions.[21,22] Immunofluorescence demonstrated spatial colocalization of CSF-1R with amylase-positive acinar structures (Figure 3A), supporting the feasibility of acinar-intrinsic responsiveness. Nevertheless, contributions from infiltrating myeloid populations remain plausible. Prior work has highlighted the role of damage-associated molecular patterns and innate immune signaling in linking acinar injury to macrophage activation during AP.[11–13] Thus, a dual-compartment model is conceivable in which IL-34 acts both on stressed acinar cells and on macrophage-lineage cells to sustain inflammatory amplification.

To extend mechanistic inference beyond correlative signaling changes, IL-34 overexpression was employed. Elevated IL-34 enhanced amylase release and cytokine secretion (Figure 4C and D) and was accompanied by increased nuclear p65 localization and p-ERK fluorescence (Figure 4E), supporting activation of ERK/NF-κB signaling downstream of IL-34. Two-way ANOVA analysis revealed significant genotype and treatment effects, with a significant genotype × treatment interaction for IL-34 secretion (Figure 4G). These findings suggest that celastrol modulates both IL-34 abundance and downstream signaling activity. Previous studies have shown that celastrol suppresses NF-κB and MAPK signaling pathways in inflammatory settings,[25,36,37] and the present results are consistent with modulation of these pathways in AP.

From a translational perspective, celastrol in the present study primarily serves as a pharmacological probe to evaluate the druggability of the IL-34/CSF-1R axis. Although celastrol has demonstrated anti-inflammatory efficacy in multiple disease models, its clinical development has been constrained by solubility limitations and potential systemic toxicities. Comprehensive toxicological evaluation will be required in future investigations to assess long-term safety and translational feasibility.[25,29] Exploratory molecular docking suggests structural compatibility between celastrol and IL-34/CSF-1R related domains; however, in the absence of direct biophysical validation, these results should be interpreted as hypothesis-generating rather than definitive evidence of direct binding.

An additional observation was the partial discordance between IL-34 mRNA and protein levels. Such divergence is compatible with post-transcriptional regulatory mechanisms influencing cytokine abundance.[40] While not central to the primary mechanistic conclusions, this finding suggests additional regulatory checkpoints that may influence IL-34 bioavailability during pancreatic inflammation.

Taken together, the present data support a model in which IL-34 protein is induced during acute pancreatic injury, accompanied by activation of CSF-1R associated ERK/NF-κB signaling, thereby contributing to inflammatory amplification. Celastrol treatment is associated with attenuation of this signaling cascade and reduction of acinar inflammatory outputs, positioning the IL-34/CSF-1R axis as a potentially modifiable inflammatory pathway in experimental AP.

## Limitations

Despite these findings, several limitations warrant consideration. First, the interaction between celastrol and the IL-34/CSF-1R complex was characterized through exploratory molecular docking; direct biophysical validation and molecular dynamics simulations are required to confirm precise binding kinetics. Second, while gain of function assays established the pro-inflammatory role of IL-34, future studies utilizing genetic deletion or neutralizing antibodies will be essential to define its absolute indispensability in AP progression. Third, the present study focused on early-phase inflammatory modulation via prophylactic celastrol administration. To evaluate true clinical potential, subsequent investigations must address therapeutic (post-injury) paradigms, long-term regenerative outcomes, and comprehensive toxicological profiles across diverse AP models. Finally, clarifying the cell-type-specific contributions of CSF-1R, distinguishing acinar-intrinsic signaling from infiltrating macrophage effects, will further refine our understanding of the pancreatic inflammatory niche.

## Conclusion

In conclusion, the present study implicates the IL-34/CSF-1R axis as a previously uncharacterized contributor to inflammatory amplification in experimental acute pancreatitis. Our data demonstrate that celastrol treatment was associated with attenuation of pancreatic injury and acinar inflammatory outputs in vivo and in vitro, accompanied by suppression of IL-34–dependent ERK/NF-κB signaling activation. While celastrol primarily serves as a pharmacological probe in this context, given its known pharmacokinetic limitations and potential toxicity, these findings provide mechanistic support for the concept that targeting IL-34/CSF-1R signaling may represent a viable therapeutic strategy. Collectively, the study expands current understanding of inflammatory regulation in AP and identifies IL-34 associated signaling as a potentially druggable inflammatory node warranting further investigation.

## Supportive Findings in Supplementary Figures

Supplementary Figure S1A documents that IL-34 mRNA does not fully mirror protein-level changes across conditions, supporting possible post-transcriptional regulation. Supplementary Figure S1B provides additional CSF-1R immunofluorescence in AR42J cells, complementing the acinar CSF-1R localization shown in Figure 3A. Supplementary Figure S1C–D include pancreatic IL-34 immunofluorescence and supportive pp65/p-ERK1/2 immunohistochemistry. Supplementary Figure S2 presents representative AR42J immunofluorescence images (WT) for IL-34, pp65, and p-ERK1/2 under PD98059/PDTC/celastrol conditions. Supplementary Figure S3 shows representative in silico docking poses of celastrol with IL-34 and CSF-1R as supportive structural context.

## Abbreviations

AMY, amylase; ANOVA, analysis of variance; AP, acute pancreatitis; CID, compound identifier; CSF-1R, colony-stimulating factor-1 receptor; DAMPs, damage-associated molecular patterns; DAPI, 4′,6-diamidino-2-phenylindole; DMSO, dimethyl sulfoxide; ELISA, enzyme-linked immunosorbent assay; ERK, extracellular signal-regulated kinase; FBS, fetal bovine serum; GAPDH, glyceraldehyde-3-phosphate dehydrogenase; HE, hematoxylin and eosin; IHC, immunohistochemistry; IF, immunofluorescence; IL-34, interleukin-34; IL-6, interleukin-6; MODS, multiple organ dysfunction syndrome; NF-κB, nuclear factor kappa B; OE, overexpression; PBS, phosphate-buffered saline; PDTC, pyrrolidine dithiocarbamate; PD98059, MEK/ERK pathway inhibitor; RIPA, radioimmunoprecipitation assay buffer; RT-qPCR, real-time quantitative polymerase chain reaction; SAP, severe acute pancreatitis; SD, Sprague Dawley; SDS-PAGE, sodium dodecyl sulfate–polyacrylamide gel electrophoresis; SIRS, systemic inflammatory response syndrome; TNF-α, tumor necrosis factor alpha.

## Data Sharing Statement

Data will be made available on request.

## Ethics Approval

All animal procedures were approved by the Animal Ethics Committee of Lanzhou University Second Hospital (approval No. D2024-227) and carried out in accordance with the ARRIVE guidelines.

## Acknowledgments

The authors gratefully acknowledge the Cuiying Biomedical Research Center, Second Hospital & Clinical Medical School of Lanzhou University, for providing experimental platforms and technical support.

## Author Contributions

Yang Yang contributed to conceptualization, methodology, investigation, formal analysis, and writing original draft preparation. Xiang-li Ma contributed to writing review & editing and validation. Yu-jie Lin contributed to conceptualization and data curation. Yue Mo contributed to visualization and software. Yao-qi Xu contributed to software and formal analysis. Bei Zhang contributed to data curation and visualization. Xu Fu contributed to methodology and supervision. Ying-zhen Wang contributed to supervision, project administration, funding acquisition, and writing review & editing. All authors made a significant contribution to the work reported, whether that is in the conception, study design, execution, acquisition of data, analysis and interpretation, or in all these areas; took part in drafting, revising or critically reviewing the article; gave final approval of the version to be published; have agreed on the journal to which the article has been submitted; and agree to be accountable for all aspects of the work.

## Funding

This work was supported by a grant from the Chinese Natural Science Foundation (82460386), Gansu Provincial Natural Science Foundation (21JR7RA396) and Innovation and Entrepreneurship Talent Project of Lanzhou (2020-RC-96). China.

## Disclosure

The authors have no competing interests to declare.

## References


1. Mayerle J, Sendler M, Hegyi E, Beyer G, Lerch MM, Genetics S-TM. Cell biology, and pathophysiology of pancreatitis. *Gastroenterology*. 2019;156(7):1951–1968e1. doi:10.1053/j.gastro.2018.11.081
2. Tenner S, Vege SS, Sheth SG, et al. American College of Gastroenterology guidelines: management of acute pancreatitis. *Am J Gastroenterol*. 2024;119(3):419–437. doi:10.14309/ajg.0000000000002645
3. Boxhoorn L, Voermans RP, Bouwense SA, et al. Acute pancreatitis. *Lancet*. 2020;396(10252):726–734. doi:10.1016/S0140-6736(20)31310-6
4. Lee PJ, Papachristou GI. New insights into acute pancreatitis. *Nat Rev Gastroenterol Hepatol*. 2019;16(8):479–496. doi:10.1038/s41575-019-0158-2
5. Mihoc T, Latcu SC, Secasan CC, et al. Pancreatic morphology, immunology, and the pathogenesis of acute pancreatitis. *Biomedicines*. 2024;12(11):2627. doi:10.3390/biomedicines12112627
6. Trikudanathan G, Yazici C, Evans Phillips A, Forsmark CE. Diagnosis and management of acute pancreatitis. *Gastroenterology*. 2024;167(4):673–688. doi:10.1053/j.gastro.2024.02.052
7. Zhang XB, Fan YB, Jing R, et al. Gastroenteropancreatic neuroendocrine neoplasms: current development, challenges, and clinical perspectives. *Mil Med Res*. 2024;11(1):35. doi:10.1186/s40779-024-00535-6
8. Shen Q, Wang S, Wu K, et al. Identification of Grb2 protein as a potential mediator of macrophage activation in acute pancreatitis based on bioinformatics and experimental verification. *Front Immunol*. 2025;16:1575880. doi:10.3389/fimmu.2025.1575880
9. Siriviriyakul P, Sriko J, Somanawat K, Chayanupatkul M, Klaikeaw N, Werawatganon D. Genistein attenuated oxidative stress, inflammation, and apoptosis in L-arginine induced acute pancreatitis in mice. *BMC Complement Med Ther*. 2022;22(1):208. doi:10.1186/s12906-022-03689-9
10. Gu A, Li J, Qiu S, et al. Pancreatic cancer environment: from patient-derived models to single-cell omics. *Mol Omics*. 2024;20(4):220–233. doi:10.1039/d3mo00250k
11. Eppensteiner J, Davis RP, Barbas AS, Kwun J, Lee J. Immunothrombotic activity of damage-associated molecular patterns and extracellular vesicles in secondary organ failure induced by trauma and sterile insults. *Front Immunol*. 2018;9:190. doi:10.3389/fimmu.2018.00190
12. Hoque R, Sohail M, Malik A, et al. TLR9 and the NLRP3 inflammasome link acinar cell death with inflammation in acute pancreatitis. *Gastroenterology*. 2011;141(1):358–369. doi:10.1053/j.gastro.2011.03.041
13. Watanabe T, Kudo M, Strober W. Immunopathogenesis of pancreatitis. *Mucosal Immunol*. 2017;10(2):283–298. doi:10.1038/mi.2016.101
14. Lee B, Zhao Q, Habtezion A. Immunology of pancreatitis and environmental factors. *Curr Opin Gastroenterol*. 2017;33(5):383–389. doi:10.1097/MOG.0000000000000387
15. Nakamichi Y, Udagawa N, Takahashi N. IL-34 and CSF-1: similarities and differences. *J Bone Miner Metab*. 2013;31(5):486–495. doi:10.1007/s00774-013-0476-3
16. Zorena K, Jachimowicz-Duda O, Waz P. The cut-off value for interleukin 34 as an additional potential inflammatory biomarker for the prediction of the risk of diabetic complications. *Biomarkers*. 2016;21(3):276–282. doi:10.3109/1354750X.2016.1138321
17. Tang F, Hou XF, Cheng Y, et al. Longitudinal associations between serum IL-34 with severity and prognosis in community-acquired pneumonia patients. *Respir Investig*. 2024;62(2):223–230. doi:10.1016/j.resinv.2023.12.008
18. Munoz-Garcia J, Cochonneau D, Teletchea S, et al. The twin cytokines interleukin-34 and CSF-1: masterful conductors of macrophage homeostasis. *Theranostics*. 2021;11(4):1568–1593. doi:10.7150/thno.50683
19. Baghdadi M, Umeyama Y, Hama N, et al. Interleukin-34, a comprehensive review. *J Leukoc Biol*. 2018;104(5):931–951. doi:10.1002/JLB.MR1117-457R
20. Baghdadi M, Endo H, Tanaka Y, Wada H, Seino KI. Interleukin 34, from pathogenesis to clinical applications. *Cytokine*. 2017;99:139–147. doi:10.1016/j.cyto.2017.08.020
21. Kai K, Iwamoto T, Zhang D, et al. CSF-1/CSF-1R axis is associated with epithelial/mesenchymal hybrid phenotype in epithelial-like inflammatory breast cancer. *Sci Rep*. 2018;8(1):9427. doi:10.1038/s41598-018-27409-x
22. Cersosimo F, Lonardi S, Ulivieri C, et al. CSF-1R in cancer: more than a myeloid cell receptor. *Cancers*. 2024;16(2):282. doi:10.3390/cancers16020282
23. Doke M, Álvarez-cubela S, Klein D, et al. Dynamic scRNA-seq of live human pancreatic slices reveals functional endocrine cell neogenesis through an intermediate ducto-acinar stage. *Cell Metabolism*. 2023;35(11):1944–1960.e7. doi:10.1016/j.cmet.2023.10.001
24. Corson TW, Crews CM. Molecular understanding and modern application of traditional medicines: triumphs and trials. *Cell*. 2007;130(5):769–774. doi:10.1016/j.cell.2007.08.021
25. Shi J, Li J, Xu Z, et al. Celastrol: a review of useful strategies overcoming its limitation in anticancer application. *Front Pharmacol*. 2020;11:558741. doi:10.3389/fphar.2020.558741
26. Zhang T, Rao Q, Dai M, Wu ZE, Zhao Q, Li F. Tripterygium wilfordii protects against an animal model of autoimmune hepatitis. *J Ethnopharmacol*. 2023;309:116365. doi:10.1016/j.jep.2023.116365
27. Yan CY, Ouyang SH, Wang X, et al. Celastrol ameliorates Propionibacterium acnes/LPS-induced liver damage and MSU-induced gouty arthritis via inhibiting K63 deubiquitination of NLRP3. *Phytomedicine*. 2021;80:153398. doi:10.1016/j.phymed.2020.153398
28. Guan Y, Cui ZJ, Sun B, Han LP, Li CJ, Chen LM. Celastrol attenuates oxidative stress in the skeletal muscle of diabetic rats by regulating the AMPK-PGC1alpha-SIRT3 signaling pathway. *Int J Mol Med*. 2016;37(5):1229–1238. doi:10.3892/ijmm.2016.2549
29. Shandra O, Wang Y, Coles LD, et al. Efficacy and tolerability of celastrol and edaravone in the multiple-hit rat model of infantile spasms. *Epilepsy Behav*. 2025;162:110159. doi:10.1016/j.yebeh.2024.110159
30. Walker DG, Tang TM, Lue LF. Studies on colony stimulating factor receptor-1 and ligands colony stimulating factor-1 and Interleukin-34 in Alzheimer's disease brains and human microglia. *Front Aging Neurosci*. 2017;9:244. doi:10.3389/fnagi.2017.00244
31. Zhang D, Li M, Dong Y, et al. 1alpha,25-Dihydroxyvitamin D3 up-regulates IL-34 expression in SH-SY5Y neural cells. *Innate Immun*. 2017;23(7):584–591. doi:10.1177/1753425917725391

32. Zhang L, Wang W, Chen T, et al. SAMHD1 dysfunction induces IL-34 expression via NF-kappaB p65 in neuronal SH-SY5Y cells. *Mol Immunol*. 2024;168:1–9. doi:10.1016/j.molimm.2024.02.003
33. Wildi S, Kleeff J, Mayerle J, et al. Suppression of transforming growth factor β signalling aborts caerulein induced pancreatitis and eliminates restricted stimulation at high caerulein concentrations. *Gut*. 2007;56(5):685–692. doi:10.1136/gut.2006.105833
34. Lv J-M, Pan Y-J, Wang X, et al. Perampanel regulates neuroinflammation and ferroptosis via activating FSP1 following brain ischemia. *J Inflamm Res*. 2025;18:14423–14437. doi:10.2147/JIR.S544785
35. Mederos MA, Reber HA, Girgis MD. Acute pancreatitis: a review. *JAMA*. 2021;325(4):382–390. doi:10.1001/jama.2020.20317
36. Jing M, Yang J, Zhang L, et al. Celastrol inhibits rheumatoid arthritis through the ROS-NF-kappaB-NLRP3 inflammasome axis. *Int Immunopharmacol*. 2021;98:107879. doi:10.1016/j.intimp.2021.107879
37. An SY, Youn GS, Kim H, Choi SY, Park J. Celastrol suppresses expression of adhesion molecules and chemokines by inhibiting JNK-STAT1/NF-kappaB activation in poly(I:C)-stimulated astrocytes. *BMB Rep*. 2017;50(1):25–30. doi:10.5483/bmbrep.2017.50.1.114
38. Xu WD, Huang AF, Fu L, Liu XY, Su LC. Targeting IL-34 in inflammatory autoimmune diseases. *J Cell Physiol*. 2019;234(12):21810–21816. doi:10.1002/jcp.28946
39. Wang F, Min HS, Shan H, et al. IL-34 aggravates steroid-induced osteonecrosis of the femoral head via promoting osteoclast differentiation. *Immune Netw*. 2022;22(3):e25. doi:10.4110/in.2022.22.e25
40. He C, Sidoli S, Warneford-Thomson R, et al. High-resolution mapping of RNA-binding regions in the nuclear proteome of embryonic stem cells. *Mol Cell*. 2016;64(2):416–430. doi:10.1016/j.molcel.2016.09.034